International journal of Engineering Research-Online
A Peer Reviewed International Journal
Articles available online http://www.ijoer.in

Vol.2., Issue.6., 2014

RESEARCH ARTICLE

ISSN: 2321-7758

SPECTRAL STUDIES OF MAGNESIUM DOPED NICKEL AND ZINC NANOFERRITES

M.S. SUBBA RAJU

Sr. Lecturer in Physics, Mrs.A.V.N.College, Visakhapatnam, Andhra Pradesh

Article received:20/11/2014 | Article Revised on: 21/12/2014 | Article Accepted on:31/12/2014

ABSTRACT

Magnesium substituted nickel zinc nano ferrite samples $Mg_x\ Zn_{0.2}\ Ni_{0.2}\ Fe_{2-x}\ O_4$ (where x=0.0, 0.2, 0.4) have been synthesized by sol-gel auto combustion method. X-ray diffraction (XRD) and infrared spectroscopy (FTIR) revealed that the obtained powders have a single phase of cubic spinel structure. The crystallite sizes calculated from XRD data have been confirmed using transmission electron microscopy (TEM) showing that the powders are consisting of nanosized grains with an average size range 39-42 nm. The SEM images show the morphology of the samples as spherical shaped particles in agglomeration. Lattice parameter decreases with increasing Mg concentration, due to the smaller ionic radius of Mg^{2+} ion. The main absorption bands of spinel ferrite have appeared through IR absorption spectra recorded in the range of 300–700 cm^{-1}. The Magnesium concentration dependence of lattice parameters obeys Vegard's law. X-ray diffraction and FTIR data reveals the formation of cubic structure phase.

Key Words: Nanoferrites, Magnesium doping, Spectral studies, XRD, SEM, TEM,FT-IR

1.0 Introduction

Nanomaterials are cornerstones of nanoscience and nanotechnology. Nanostructured science and technology is a broad and interdisciplinary area of research and development activity. Nanocrystalline spinel ferrites are the important class of materials having a variety of electronic, magnetic and catalytic properties. The ferrite nanoparticles are having large number of applications in different areas such as biomedical, ferrofluid, magnetic media, microwave, magnetocaloric refrigeration and gas sensors[1]. The ferrites are semiconductor materials with the formula MFe_2O_4, where M can be a divalent metal cation[2]. Ferrites are regarded as better magnetic materials than pure metals because of their high resistivity, lower cost, easier manufacture and superior magnetization properties. Ferrites are extensively used in radar, audio-video and digital recording, bubble devices, memory cores of computers, satellite communication and microwave devices[3]. Nanophase ceramics are of particular interest because they are more ductile at elevated temperatures as compared to the coarse-grained ceramics. Nanostructured semiconductors are known to show various non-linear optical properties. The method of preparation of nano ferrites with different metal ions modifies the

distribution of ions in the ferrite structure. To obtain low cost nano particles of Magnesium ferrite powders, several methods of syntheses are available. In the present study, the influence of Ni^{2+} and Zn^{2+} on the constitution and magnetic properties of nano Mg^{2+} ferrite particles prepared by sol-gel methods are being reported. This paper focuses on the synthesis of $Mg_x\ Zn_{0.2}\ Ni_{0.2}\ Fe_{2-x}\ O_4$ (where x=0.0, 0.2, 0.4) nanoparticles using the co-precipitation method, their characterization by means of powder X-ray diffraction, Scanning Electron Microscopy (SEM), FTIR, Transmission Electron Microscope (TEM), and the determination of the dielectric properties and the magnetic behaviour of $Mg_x\ Zn_{0.2}\ Ni_{0.2}\ Fe_{2-x}\ O_4$ (where x=0.0, 0.2, 0.4) nanoparticles.

2.0 Materials and Method

All the chemicals were purchased from Merck India, Sd fine chemicals and were used without extra purification (99.9% purity). Chemicals used in the synthesis were $(Ni(NO_3)_2.6H_2O)$, magnesium nitrate $(Mg(NO_3)_2.6H_2O)$, zinc nitrate $(Zn(NO_3)_2.6H_2O)$, ferric nitrate $(Fe(NO_3)_3.9H_2O)$ and citric acid $(C_6H_8O_7)$. The stoichiometric amounts of metal nitrates and citric acid were dissolved in double distilled water. Metal nitrate solutions were mixed with citric acid solution in 1:1 molar ratio of nitrate to citric acid. The pH of the solution was maintained at 7.0 using ammonia solution. Then the solution was heated at 100°C to transform into a thick gel. Thereafter, the gel ignited and burnt with glowing flints yielding loose ferrite powder. The as-burnt powder was granulated using 15% polyvinyl alcohol as a binder and was pressed to form pellets (10mm diameter) and toroidal rings (30mm outer diameter, 10mm inner diameter and 3mm thickness) by applying a pressure of 10 ton cm^{-2}. These specimens were pre-sintered at 700°C for 3h in a programmable conventional furnace to expel the binder and were then subjected to final sintering at 800°C for 3h using the above mentioned furnace at a heating rate of 5°C/min. The samples were furnace cooled.

2.1 Characterizations

$Mg_x\ Zn_{0.2}\ Ni_{0.2}\ Fe_{2-x}\ O_4$ (where x=0.0, 0.2, 0.4) formation was confirmed by the XRD (Philips) with Cu Kα (λ=1.5405Å) results. Philips CM 200 transmission electron microscope is used to record TEM images and microscope is operated at 200 kV with a resolution of 0.23 nm. The FTIR spectra of the ferrite samples as pellets in KBr were recorded by SHIMADZU FTIR spectrophotometer in the frequency range of 400 to 600 cm^{-1}. SEM studies were carried out using JEOL, JSM- 67001.

3.0 Results and Discussion

3.1 TEM analysis: The particle size, shape and size distribution are important morphological characteristics for a nano scaled material[4]**.** Transmission electron microscopy (TEM) was employed to visualize the size, shape and to confirm the nano crystalline nature of the synthesized Mg^{2+} doped nano ferrites. Figure 1 shows the typical TEM images of the synthesized Mg-Zn-Ni nanoparticles. Also it is noticed that the ferrite nano particles are well defined with polygonal octahedral and tetrahedral and spherical shapes .These are well joined. The whole surface of the grid was covered with dense magnesium-ferrite nanoparticles. This type of joining may find important application as building block for magnetic nanostructures. The particle size is decreases with increase of Mg concentration (x=0.2). The whole surface of the grid covered with less number of different sizes of cores domains of nanoparticles because of doping of Mg^{2+} into the Zn-Ni ferrite system which suggest that ferromagnetic behaviour is reducing and super-paramagnetic behaviour in with increasing the increase of doping. The cores are in the rod shape. Further some of the grains are over lapped and could not be identified separately. When x = 0.4 the particle size is further reduced and few number of large domains appeared. Some of them are also in the lungs shape. This further confirms that ferromagnetic behaviour has completely disappeared and only paramagnetic behaviour of the compound is observeded. The agglomeration of nano particles is usually explained as a common way to minimize their surface free energy in nano materials. TEM images show the presence of particles which are spherically cubic shaped crystallites of size approximately 39 nm and varies to less than 40 nm with an increase in Mg^{2+} ion substitution. This corroborates well with the results obtained from XRD according to the

Scherrer's formula. Agglomerated particles as well as separated ones are observed in the images of the sample.

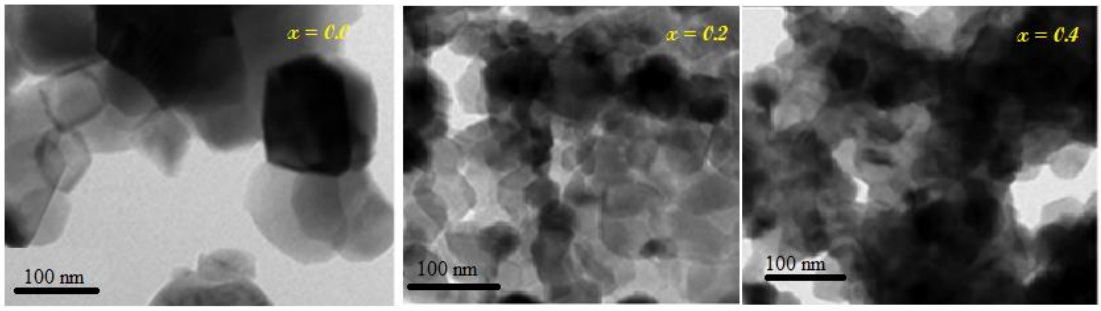

Figure 1: TEM micrographs of nano crystalline $Mg_x\ Zn_{0.2}\ Ni_{0.2}\ Fe_{2-x}\ O_4$ (where x=0.0, 0.2, 0.4) nanoferrites

3.2 XRD Analysis: The X-Ray Diffraction pattern for the sample $Mg_x\ Zn_{0.2}\ Ni_{0.2}\ Fe_{2-x}\ O_4$ (where x=0.0, 0.2, 0.4) is shown in Figure 2. The average crystallite size for each composition was calculated from the full width at half maximum intensity for (311) plain using Scherrer's formula (equation 1)[v]. The values of the lattice parameter were determined by using the following equation.

$$a = \frac{d}{\sqrt{h^2+k^2+l^2}} \quad \text{....(1)}$$

Where, $h.\ k.\ l$ are miller indices..

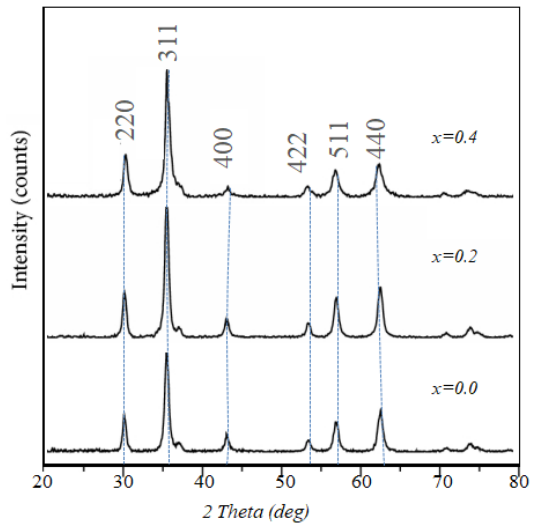

Figure 2. X-ray Diffraction Pattern for $Mg_x\ Zn_{0.2}\ Ni_{0.2}\ Fe_{2-x}\ O_4$ (where x=0.0, 0.2, 0.4)

In the present investigation, The bulk value of the lattice constant for $Mg_{0.4}\ Zn_{0.2}\ Ni_{0.2}\ Fe_{1.6}O_4$ reported as 8.6342Å and it was observed that decrease in the lattice constant. A similar decrease in the lattice constant was reported by Arulmurugan *et al*.(2008)[vi]. This decrease in the lattice constant may be due to change in the cation distribution between A site and B site. in the nano regime[vii]. However there is an increase in the lattice constant with the increase in the Mg content. This increase in the lattice constant is due to larger ionic radii of the Mg^{2+} (0.65 Å) as compared to Fe^{3+} (0.63Å) ions. The intensities of the planes (220) and (440) are more sensitive to any change in cation on tetrahedral A sites and octahedral B sites respectively. Mg^{2+}ions and Zn^{2+} ions have chemical affinity towards tetrahedral A sites. Mean while Mg^{2+} and Fe^{3+} ions have, preferences for both tetrahedral A sites and octahedral B sites respectively. Since the X-Ray scattering factor for Mg^{2+}ion is significantly high as compared to those of the other cations, the intensities of the (220) plane and (440) plane increases with increasing Mg^{2+}ion concentration. This shows that Mg^{2+}ions occupy tetrahedral A sites and octahedral B sites in the nano dimension against their chemical preference for A site as observed in bulk samples.

3.3 SEM Analysis: The samples needed a coating of gold for SEM analysis for the avoidance of charging effect. The morphology and the size distribution of the $Mg_x\ Zn_{0.2}\ Ni_{0.2}\ Fe_{2-x}\ O_4$ (where x=0.0, 0.2, 0.4) nanoparticles were determined using SEM. Typical SEM images of $Mg_x\ Zn_{0.2}\ Ni_{0.2}\ Fe_{2-x}\ O_4$ (where x=0.0, 0.2, 0.4)

synthesized particles are shown in Figure 3. SEM micrograph depicts that the samples contain micrometrical aggregation of tiny particles. The existence of high dense agglomeration indicates that pore free crystallites are present on the surface. The SEM images show the agglomerated form of $Mg_x Zn_{0.2} Ni_{0.2} Fe_{2-x} O_4$ (where x=0.0, 0.2, 0.4) nanoparticles. As the nanoparticles possess high surface energies, they tend to agglomerate and grow into larger assemblies.

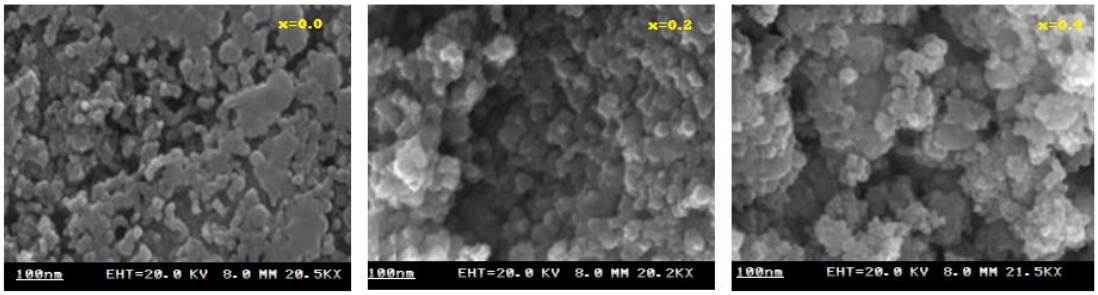

Figure 3: SEM micrographs of nano crystalline $Mg_x Zn_{0.2} Ni_{0.2} Fe_{2-x} O_4$ (where x=0.0, 0.2, 0.4) nanoferrites

3.4 FT IR Analysis: The FTIR spectra of nickel substituted lithium ferrites measured in the frequency range of 400 cm^{-1}-4000 cm^{-1} were shown in Fig. 4. From the figures, it is noticeable that the three main absorption bands appeared common in almost all spinel ferrites of the ferrite system under investigation. The spectrum elucidates the position of the ions in the crystal structure and their vibration modes, which represents the various ordering positions on the structural properties of the synthesized compound. The FTIR spectrum of the $Mg_x Zn_{0.2} Ni_{0.2} Fe_{2-x} O_4$ (where x=0.0, 0.2, 0.4) nanoparticles was taken to determine the chemical structure of the sample, the FTIR spectrum was observed above the frequency range of 4000-500 cm-1 as shown in Figure 4. The decomposition of hydroxide to oxide phase for the formation of spinel ferrites was well reflected in the FTIR spectrum. It has been reported that the IR bands of solids are usually attributed to the vibration of ions in the crystal lattice. The bands at 552cm^{-1} and 464 cm^{-1} represented tetrahedral and octahedral modes of $Mg_x Zn_{0.2} Ni_{0.2} Fe_{2-x} O_4$ (where x=0.0, 0.2, 0.4), respectively[viii].Normal ferrites both absorption bands depend on the nature of octahedral M–O stretching vibration and nature of tetrahedral M–O stretching vibration. Two main frequency bands, namely, high frequency band (around 580 cm^{-1}) and low frequency band (around 430 cm^{-1}) reveals formation ferrite. These two observed bands (v_1 and v_2) correspond to the intrinsic vibrations of tetrahedral and octahedral Fe^{3+}–O_2 complexes,respectively.

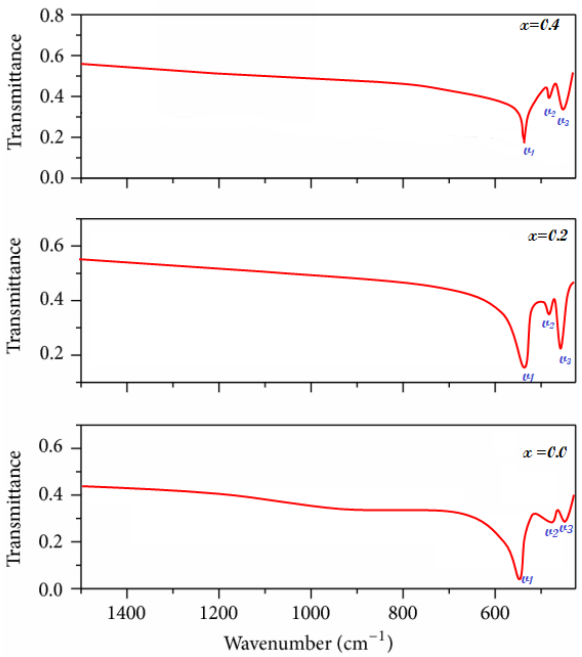

Figure 4: FTIR images of of nano crystalline $Mg_x Zn_{0.2} Ni_{0.2} Fe_{2-x} O_4$ (where x=0.0, 0.2, 0.4) nanoferrites

In ferrites the metal ions are situated at two sublattices named tetrahedral (A) site and octahedral (B) site. This confirms the spinel structure of the prepared ferrite

compositions. Similar reports were observed by Zahi and Pathak[ix,x]. The observed larger v_1 values of the prepared ferrites compared to the v_2 values indicates the normal mode of vibration in these ferrites. This is because of shorter bond length of A-site compared to that of B site. According to Tarte[xi], the recorded band v_3 indicates the presence of LieO complexes on the octahedral sites. The intensity of this band goes on decreasing with increase in the nickel substitution in the system.

4.0 CONCLUSIONS

The paper thoroughly discussed the synthesis of Mg_x $Zn_{0.2}$ $Ni_{0.2}$ Fe_{2-x} O_4 (where x=0.0, 0.2, 0.4) nanoparticles by the employment of co Sol-gel method. The fact that the Mg_x $Zn_{0.2}$ $Ni_{0.2}$ Fe_{2-x} O_4 nanoparticles belonged to the cubic spinal structure was established by XRD. FTIR spectrum also supported the formation of Mg_x $Zn_{0.2}$ $Ni_{0.2}$ Fe_{2-x} O_4 nanoparticles. That the nanoparticles agglomerated to form spherical-shaped particles was also confirmed and made clear by the SEM analysis. The average particle size of Mg_x $Zn_{0.2}$ $Ni_{0.2}$ Fe_{2-x} O_4 nanoparticles was found to be 40 nm. The X-ray intensity of the (440) plane and (220) plane increases with increasing Mg^{2+} ion concentration. This shows that Mg^{2+}ions occupy both tetrahedral A site and octahedral B sites in the nano dimension. The line width Mg content. This is due to the increase in the super exchange interaction between Fe^{2+} and Fe^{3+} ions at octahedral B sites.

References

[1]. T. Tanaka, R. Shimazu, H. Nagai, M. Tada, T. Nakagawa, A. Sandhu, H. Handa, M. Abe, Preparation of spherical and uniformsized ferrite nanoparticles with diameters between 50 and 150 nm for biomedical applications, J. Magn. Magn. Mater. 321 (2009) 1417–1420.

[2]. S. Rahman, K. Nadeem, M.A. Rehman, M. Mumtaz, S. Naeem, I.L. Papst, Structural and magnetic properties of ZnMg-ferrite nanoparticles prepared using the co-precipitation method, Ceram. Int. 39 (2013) 5235–5239

[3]. S. Hajarpour, K. Gheisari, A.H. Raouf, Characterization of nanocrystalline Mg0.6Zn0.4Fe2O4 soft ferrites synthesized by glycine–nitrate combustion process, J. Magn. Magn. Mater. 329 (2013) 165–169.

[4]. Kumar V, Rana A, Kumar N, Pant RP. Investigations on controlled size precipitated cobalt ferrite nano particles. Int JApplCeramTechnol 2011;8:120

[5]. Cullity R. D., (1996), Elements of X-ray Diffraction. Addision-Wesley Public Co. INC; 42

[6]. Arulmurugan R., Jeyadevan B., Vaidyanayhan G., Sendhilnathan S., (2008), Effect of Zinc substitution on Co-Zn and Mn-Zn ferrite nanoparticles prepared by co-precipitation. *J. Magn. Magn. Mater*. 288: 470-477

[7]. Ladgaonkar B. P., Vaingainkar A. S., (1998), X-ray diffraction investigation of cation distribution in CdCu1-xFe2O4, *Mater. Chem. Phys*. 56: 280-283

[8]. Guo L, Shen X, Meng X, Feng Y. Effect of Sm3+ ions doping on structure and magnetic properties of nanocrystalline NiFe2O4 fibers. *Journal of Alloys and Compounds*. 2010;490(1-2):301-306

[9]. Pathak TK, Vasoya NH, Lakhani VK, Modi KB. 2010. Structural and magnetic phase evolution study on needle-shaped nanoparticles of magnesium ferrite. Ceram Int 36(1): 275-281. doi: 10.1016/j. ceramint.2009.07.023

[10]. Zahi S. 2010. Synthesis, permeability and microstructure of the optimal Nickel-Zinc ferrites by sol-gel route. Journal of Electromagnetic Analysis & Applications 2(1): 56-62. doi: 10.4236/jemaa.2010.21009

[11]. Tarte P. Infra-red spectrum and tetrahedral coordination of lithium in the spinel LiCrGeO4. Acta Crystallogr 1963;16:228